Synthesis and Characterization of Mixed Methyl/Allyl Monolayers on Si(111)†

Leslie E. O'Leary, Erik Johansson, Bruce S. Brunschwig, and Nathan S. Lewis*

Beckman Institute and Kavli Nanoscience Institute, California Institute of Technology, Pasadena, California 91125

Received: November 30, 2009; Revised Manuscript Received: July 12, 2010

The formation of mixed methyl/allyl monolayers has been accomplished through a two-step halogenation/alkylation reaction on Si(111) surfaces. The total coverage of alkylated Si, the surface recombination velocities, and the degree of surface oxidation as a function of time have been investigated using X-ray photoelectron spectroscopy, Fourier-transform infrared spectroscopy, and microwave conductivity measurements. The total coverage of alkyl groups, the rate of oxidation, and the surface recombination velocities of Si(111) terminated by mixed monolayers were found to be close to those observed for $CH_3-Si(111)$ surfaces. Hence, the mixed-monolayer surfaces retained the beneficial properties of $CH_3-Si(111)$ surfaces while allowing for convenient secondary surface functionalization.

I. Introduction

Alkylated Si(111) surfaces have been widely investigated due to their desirable electrical properties and superior air stability relative to the H-terminated Si(111) surface.[1,2] In addition to several ultrahigh-vacuum techniques,[3,4] wet chemical methods for the formation of surficial Si−C bonds include radical-,[5,6] thermal-,[7] ultraviolet-[8] or white light- initiated hydrosilylation;[9] metal-catalyzed hydrosilylation;[10] two-step halogenation/alkylation;[11] electrochemical;[12] and mechano-chemical[13] processes. Hydrosilylation has been especially well developed,[14−16] facilitating incorporation of a wide range of functionalities of interest for catalysis and sensing,[14,15] as well as enabling the manipulation of surface properties and the covalent attachment of contacts.[16] Hydrosilylation cannot, however, make a surface terminated by a C_1, $CH_3-Si(111)$, group.

The $CH_3-Si(111)$ surface, which is readily prepared by a two-step halogenation/alkylation process, has been reported to exhibit exceptional passivation toward oxidation in ambient air,[17,18] essentially complete coverage of Si(111) atop sites,[19,20] low surface recombination velocity (S) values,[17] and a minimal barrier to electron tunneling.[21] However, due to the low reactivity of the $-CH_3$ moiety, facile secondary functionalization is difficult on the $CH_3-Si(111)$ surface. Accordingly, the $CH_2CHCH_2-Si(111)$ surface has been synthesized by a halogenation/alkylation procedure.[22−24] The $CH_2CHCH_2-Si(111)$ surface has good passivation properties, but the total attainable coverage of functional groups is lower than that exhibited by the $CH_3-Si(111)$ surface. Additionally, surface oxidation occurs more rapidly on the $CH_2CHCH_2-Si(111)$ surface than on the $CH_3-Si(111)$ surface.[17,23] The $CH_2CHCH_2-Si(111)$ surface does allow additional functionalization through the use of the Heck reaction or the olefin cross-metathesis reaction, but relatively low coverages of secondary functional groups are observed. For example, only ∼30% functionalization is observed for the cross-metathesis reaction, presumably due to crowding of the allyl groups on the surface.

The use of mixed monolayers (MMs) can lead to functionalized surfaces that will undergo well-defined, high-yield, secondary functionalization reactions.[25] MMs on silicon have been produced by the attachment of long-chain hydrocarbons through hydrosilylation[26−29] and through the self-assembly of silanes on oxidized silicon surfaces.[30,31] Dilution of surface functional groups, to avoid crowding, has been achieved using both of these approaches.[25,26,31−33] For example, olefin cross-metathesis proceeded for only 10−15% of all surface-bound alkenes for a surface terminated with only alkenes,[32] whereas 50% of all alkenes reacted on an MM surface that consisted of a 1:1 ratio of alkenes to unreactive alkanes. Steric hindrance and cross-coupling of surface-bound species were presumed to contribute to the low amount of functionalization observed on the pure alkene monolayers.[25,33]

In this work, we describe the preparation and properties of mixed methyl/allyl monolayers on Si(111) surfaces (MM-Si(111)). The formation of methyl/allyl MMs was confirmed using grazing-angle attenuated total reflectance infrared (GATR-IR) spectroscopy. The total surface coverage was investigated using X-ray photoelectron spectroscopy (XPS). The relative surface defect densities were investigated by surface recombination velocity measurements, and the surface oxidation over time was monitored using XPS. The goal was to prepare surfaces that had the desirable passivation and electrical properties of the $CH_3-Si(111)$ surface while also enabling facile introduction of secondary functional groups at reasonably high coverages.

II. Experimental Section

A. Materials and Methods. All chemicals were used as received. Water was obtained from a Barnstead Nanopure system and had a resistivity of ≥18.2 MΩ cm.

Float-zone grown n-type Si(111) wafers (Silicon Quest International, Santa Clara, CA), used for GATR, XPS, and transmission IR (TIR) were polished on both sides and had a resistivity of 63−77 Ω cm. Surface recombination velocity measurements were performed on double-side polished, high-purity, monocrystalline n-Si(111) wafers (Topsil, Santa Clara, CA) that had a resistivity of 4−8 kΩ cm. Surfaces were functionalized as described previously.[11,23,34,35]

1. Oxidation of and Removal of Organic Contaminants from Wafers. Si(111) wafers were cut to the appropriate size, 1 × 1 cm for XPS analysis and surface recombination velocity measurements, 1.5 × 1.5 cm for GATR-IR, and 1.5 × 3 cm

† Part of the "Michael R. Wasielewski Festschrift".

* Corresponding author. Phone: (626) 395-6335. Fax: (626) 395-8867. Address: 210 Noyes Laboratory, 127-72, California Institute of Technology, Pasadena, CA 91125. E-mail: nslewis@caltech.edu.

10.1021/jp911379c
Published on Web 08/19/2010

for TIR, and were sequentially rinsed with water, methanol, acetone, methanol, and then water. The surfaces were then cleaned at 100 °C for 5 min in a piranha solution (1:3 by volume ratio of 10.1 M H_2O_2(aq): 18 M H_2SO_4). After the piranha treatment, the wafers were slowly cooled to room temperature and rinsed with water. Care was taken not to let the wafers dry during the cleaning procedure or prior to the hydrogen-termination steps.

2. Hydrogen Termination of Si(111) Samples. Atomically smooth H−Si(111) surfaces were obtained by use of one of the two following procedures: (A) The wafers were immersed for 45 s in a 6 M aqueous hydrofluoric acid (HF(aq)) solution that had been prepared by dilution of 49% HF(aq) (semiconductor grade, Transene Company, Inc., Danvers, MA). The Si(111) samples were then removed from the HF(aq), rinsed with H_2O, and immediately immersed for 10 min into 11 M NH_4F(aq) (semiconductor grade, Transene Company, Inc., Danvers, MA). The samples were removed from the NH_4F(aq) and then rinsed with water. (B) Wafers were submerged for 18 s in buffered HF(aq) (semiconductor grade, Transene Company, Inc., Danvers, MA). The samples were removed and immediately placed for 17 min in 11 M NH_4F(aq). The samples were then removed from the NH_4F(aq), rinsed with water, and quickly dried under a stream of N_2(g). In either procedure, A or B, the NH_4F solution was purged with ultrahigh purity Ar for at least 25 min prior to use. The NH_4F(aq) was continuously purged during the etching process, and agitation of the sample prevented the accumulation of bubbles on the surface of the wafer.

Both processes produced atomically flat H-terminated Si(111), as indicated by TIR spectroscopy.[36] After etching, the samples were immediately introduced into a N_2(g)-purged flush box that contained less than 10 ppm of O_2(g), unless the samples were to be investigated using TIR, in which case they were placed directly into a Fourier transform infrared (FTIR) spectrometer.

3. Chlorination of H−Si(111). H−Si(111) samples were chlorinated by immersion into a saturated solution of PCl_5 (99.998% metal basis, Alfa Aesar) in chlorobenzene (Anhydrous, 99.8%, Sigma Aldrich) to which a small amount of benzoyl peroxide (Aldrich reagent grade, 97%, Sigma Aldrich) had been added. After heating to 90−95 °C for 45 min, the wafers were cooled to room temperature, removed from the chlorinating solution, and rinsed with chlorobenzene, followed by a rinse with tetrahydrofuran (THF).

4. Alkylation of Cl−Si(111) Samples. Immediately following chlorination, the samples were immersed in a 1.0 M alkylating solution (CH_3MgCl (diluted from 3.0 M in THF, Aldrich,), CH_2CHCH_2MgCl (diluted from 2.0 M in THF, Aldrich), or a mixture of the two) at 70−75 °C for 3 h. The alkylated samples were rinsed with THF, rinsed with methanol, brought out of the inert atmosphere box, and sonicated sequentially for 10 min each in THF, methanol, and water, or in methanol, acetonitrile, and then water. Regardless of the cleaning procedure, no Mg or Cl signals were observed on the surface by XPS.

5. Surface Oxidation. Samples used for the oxidation study (1 cm ×1 cm) were functionalized as described above. After the reaction workup, the samples were stored in lab air, in Fluoroware, in the dark. The samples were exposed to light only during transportation to the XPS chamber, which encompassed a total time of <1 h, relative to the cumulative elapsed 4 weeks that the samples were exposed to air.

B. Instrumentation. All FTIR spectra were collected using a Thermo Scientific Nicolet 6700 Optical Spectrometer that was equipped with a deuterated triglycine sulfate (DTGS) detector and a purified air purge. ATR spectra were recorded using the GATR accessory (Harrick Scientific Products, Inc.) in which samples were pressed against a hemispherical Ge crystal and illuminated at a fixed 65° incident angle. The aperture was maximized for 4 cm^{-1} resolution, and the throughput of the GATR accessory was 11.8% at 2500 cm^{-1}. Prior to mounting, the samples and the Ge crystal were cleaned with methyl ethyl ketone. The sample compartment was purged with purified air for at least 1 h before collection of spectra, and all spectra were averages of greater than 3000 consecutive scans. TIR spectra were collected by mounting the samples at a fixed 74° angle, as measured between the incident light and the surface normal. The sample chamber was purged with purified air for at least 1 h before collection of spectra. All of the reported TIR spectra represent averages of greater than 3000 consecutive scans.

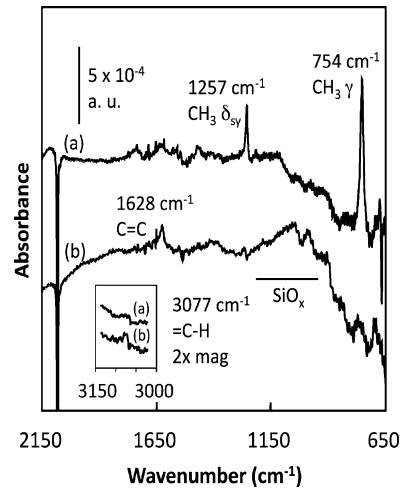

Figure 1. Transmission spectra of (a) CH_3−Si(111) and (b) CH_2CHCH_2−Si(111) referenced to the H−Si(111) surface. Characteristic CH_2CHCH_2− modes include 3077 cm^{-1} (=C−H) and 1628 cm^{-1} (C=C) stretches. The characteristic CH_3− modes used for the determination of $\theta_{Si\text{-}CH_3}$ are the 1257 cm^{-1} (δ_{sy}, umbrella) and 754 cm^{-1} (γ mode).

XPS data were collected using a Surface Science Instruments M-Probe system that has been described previously.[37] Ejected electrons were collected at an angle of 35° from the surface normal, and the sample chamber was maintained at $<5 \times 10^{-9}$ Torr. Survey scans from 0 to 1000 eV were performed to identify the elements present on the surface. High-resolution spectra were collected for the Si 2p and C 1s regions. The XPS data were analyzed using the ESCA Data Analysis Application (V2.01.01; Service Physics, Bend, OR). The monolayer (ML) thickness of oxidized Si was calculated as described previously.[34]

Photoconductivity decay measurements were made using a contactless microwave conductivity apparatus.[17,23] Electron-hole pairs were generated with a 20 ns laser pulse at 905 nm using an OSRAM laser diode with an ETX-10A-93 driver. The lifetime of the excess charge carriers was monitored via the reflected microwave radiation that was detected by a PIN diode. Samples were tested immediately after workup as well as for several days after preparation. Samples were either stored in an N_2-filled glovebox or in the dark in air. In both cases, the surface recombination velocity, S, stabilized over a few days, and reproducible trends were observed.

III. Results

Figure 1 depicts representative TIR spectra of the CH_3−Si(111) and CH_2CHCH_2−Si(111) surfaces. As observed previously, the CH_3−Si(111) surface exhibited a characteristic

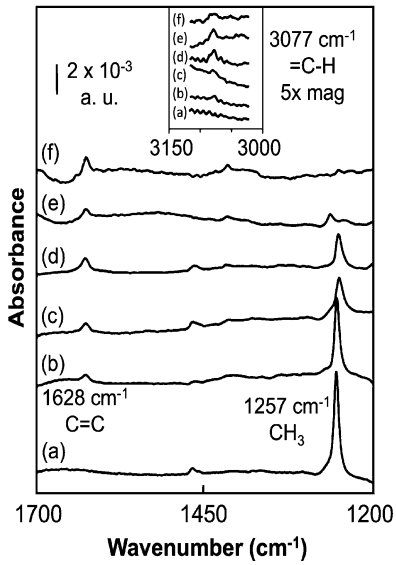

Figure 2. GATR-FTIR spectra of MM-Si(111) surfaces synthesized from solutions having $\chi_{CH_2CHCH_2MgCl}$ = (a) 0, (b) 0.02, (c) 0.10, (d) 0.15, (e) 0.50, and (f) 1 reaction solution compositions. Spectra are referenced to the H−Si(111) surface. Characteristic CH_2CHCH_2- peaks include the vibrational modes at 3077 cm^{-1} (=C−H stretch, inset) and 1628 cm^{-1} (C=C stretch). The characteristic methyl vibrational mode was observed at 1257 cm^{-1} (CH_3 umbrella, δ_{sy}). MM-Si(111) samples displayed both CH_2CHCH_2- and CH_3- vibrational modes, whereas the CH_3−Si(111) surface showed only CH_3- modes. The CH_3 umbrella mode was highly attenuated even at $\chi_{CH_2CHCH_2MgCl} = 0.15$. The peak at 1465 cm^{-1} is ascribed to the 2-butanone solvent used to clean the samples prior to GATR spectroscopy.

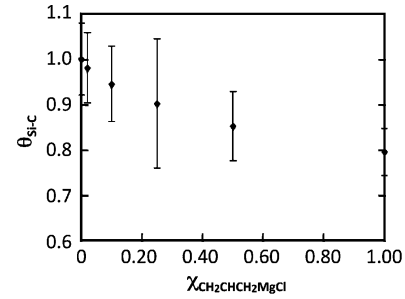

Figure 3. Fraction of C-terminated Si(111) atop sites, θ_{Si-C}, as determined using XPS, as a function of the composition of the reaction solution composition, $\chi_{CH_2CHCH_2MgCl}$. Surfaces made from solutions having $\chi_{CH_2CHCH_2MgCl} \leq 0.10$ had statistically higher θ_{Si-C} than did CH_2CHCH_2−Si(111) surfaces. The average coverages decreased rapidly as the reaction solution composition was changed toward $\chi_{CH_2CHCH_2MgCl} = 1$. Error bars are ±1 standard deviation over several (≥4) samples.

TABLE 1: Summary of MM-Si(111) Surface Coverage[a]

$\chi_{CH_2CHCH_2MgCl}$[b]	θ_{Si-C} [c]
0	1.00 ± 0.08
0.02	0.98 ± 0.08
0.10	0.95 ± 0.08
0.25	0.90 ± 0.14
0.50	0.85 ± 0.08
1	0.80 ± 0.05

[a] Values ±1 standard deviation. [b] Total Grignard reagent concentration fixed at 1.0 M. [c] Quantified using XPS spectroscopy with CH_3−Si(111) as a standard of $\theta_{Si-C} = 1.00$.

methyl umbrella mode at 1257 cm^{-1} and a CH_3 γ mode at 754 cm^{-1}, whereas the allyl-terminated Si(111) surface exhibited characteristic peaks at 3077 cm^{-1} (the =C−H stretching mode) and 1628 cm^{-1} (the C=C stretching mode).[23,38] A weak C=C−H bending mode is expected at 1420 cm^{-1}.

A. GATR-FTIR Spectroscopy. Qualitative information regarding the surface composition as a function of the composition of the reaction solution was obtained using GATR-FTIR spectroscopy. Figure 2 shows representative spectra of the mixed CH_3-/CH_2CHCH_2−Si(111) (MM-Si(111)) surfaces prepared from solutions that contained varying ratios of CH_3MgCl to CH_2CHCH_2MgCl, at a constant total Grignard reagent concentration of 1.0 M. The mole fraction of CH_2CHCH_2MgCl in the reaction solution, $\chi_{CH_2CHCH_2MgCl}$, was calculated as $\chi_{CH_2CHCH_2MgCl} = [CH_2CHCH_2MgCl]/([CH_2CHCH_2MgCl] + [CH_3MgCl])$. Peaks at 3077 cm^{-1} and 1628 cm^{-1}, previously assigned to the =C−H stretch and the C=C stretch of the allyl moiety, respectively,[23] were clearly observed for samples that were prepared using reaction solutions having $\chi_{CH_2CHCH_2MgCl} = 0.02$, 0.10, 0.15, 0.25, 0.50, 0.75 and 1.00, but not for pure CH_3−Si(111) surfaces. The CH_3- umbrella mode, at 1257 cm^{-1}, was observed for CH_3−Si(111) samples, and was seen at reduced intensity for samples prepared using reactions solutions having $\chi_{CH_2CHCH_2MgCl} = 0.02$, 0.10, 0.15, 0.25, and 0.50 (Figure 2). As expected, the CH_3 umbrella mode was not observed for surfaces prepared using only CH_2CHCH_2MgCl. While the absolute intensities in GATR-FTIR spectra are not useful for quantitative coverage determination, because the peak intensities are sensitive to the contact between the sample and the Ge crystal,[39] it is appears from the relative peak intensities of Figure 2 that the surface composition is not linearly dependent on reaction solution composition. Barring a large change in absorption cross-section of the methyl and allyl moieties with a change in surface composition, transmission FTIR spectroscopy should be useful for quantitative composition analysis. In this case, however, the vibrational modes characteristic of the allyl group are very weak. In addition, interference in the IR spectra caused by slight differences in Si wafer thickness when comparing CH_3−Si(111) to MM-Si(111) or CH_2CHCH_2−Si(111), and variation in final MM-Si(111) monolayer composition due to the variation in Grignard reagent concentrations, limited the precision with which weak signals could be quantitatively evaluated. Despite these limitations, the qualitative conclusion of transmission FTIR data (Figure S2, Supporting Information) agrees with that of the GATR-FTIR data and shows that both CH_3- and CH_2CHCH_2- groups were present on the surface, and that the MM-Si(111) monolayer compositions were not linearly dependent on the solution composition.

B. XPS Surface-Coverage Measurements. Samples prepared using CH_3MgCl are known to produce a surface in which essentially all of the Si(111) atop sites are CH_3-terminated.[19] The fractional coverage of Si(111) atop sites terminated by C-bonds, θ_{Si-C}, was calculated as $\theta_{Si-C} = \Gamma_{Si-C}/\Gamma_{Si}$ where Γ_{Si-C} is the number of Si−C bonds per area unit, and Γ_{Si} is the number of Si atop sites per area unit. To calculate θ_{Si-C}, the area of the C 1s peak assignable to Si-bonded C was compared to that of a CH_3−Si(111) surface in the XPS spectra. To account for variations in absolute signal strength, all Si-bonded C signals were normalized by the Si 2p peak area observed for each sample.[34] Figure 3 and Table 1 display θ_{Si-C} obtained by this method, as a function of $\chi_{CH_2CHCH_2MgCl}$. For monolayers prepared from CH_2CHCH_2MgCl alone, θ_{Si-C} was approximately equal to 0.80. For the pure allyl surface, θ_{Si-C} was, with 95% confidence, lower than that obtained for CH_3−Si(111) or for MM-Si(111) surfaces that were prepared from Grignard solutions with $\chi_{CH_2CHCH_2MgCl} \leq 0.10$. The errors in these measurements reflect a combination of differences in actual surface

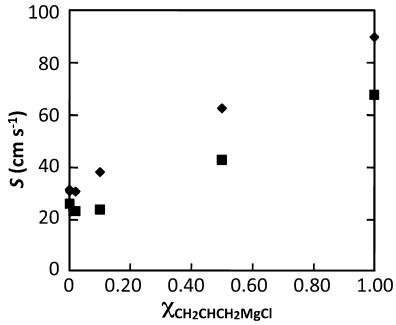

Figure 4. Plot of the surface recombination velocity (S) of MM-Si(111), $CH_3-Si(111)$, and $CH_2CHCH_2-Si(111)$ surfaces versus $\chi_{CH_2CHCH_2MgCl}$. The value of S decreased with increased CH_3MgCl in the reaction solution, and MM-Si(111) surfaces made from solutions having $\chi_{CH_2CHCH_2MgCl} = 0.02$ exhibited S values indistinguishable from those of the $CH_3-Si(111)$ surface. The squares and triangles represent two separate sets of data, and show the reproducibility in the observed trend.

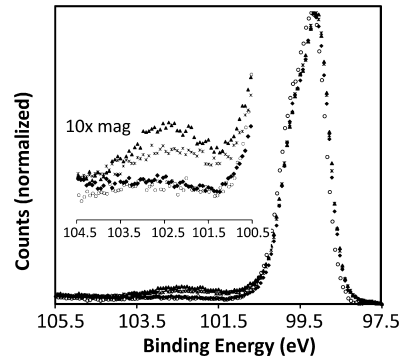

Figure 5. Si 2p region of the XP spectrum of $CH_3-Si(111)$ (○), MM-Si(111) (from solutions having $\chi_{CH_2CHCH_2MgCl} = 0.02$ (◆), and 0.10 (×)), and $CH_2CHCH_2-Si(111)$ (▲) after 4 weeks in air. After 4 weeks, the $CH_3-Si(111)$ surface and MM-Si(111) surfaces made from solutions having $\chi_{CH_2CHCH_2MgCl} = 0.02$ were nearly identical, with oxidation below the detection limit of the apparatus. The MM-Si(111) surface made from solutions having $\chi_{CH_2CHCH_2MgCl} = 0.10$ exhibited less than one-third the oxidation observed on the $CH_2CHCH_2-Si(111)$ surface.

coverage and uncertainty in the measurements, hence for surfaces with high θ_{Si-C} values the error bars may at times include values that exceed 100% coverage of Si atop sites.

C. Surface Recombination Velocity Measurements. Charge-carrier lifetimes were measured for the various MM surfaces, and the resulting lifetimes were then used to calculate surface recombination velocities and equivalent electronic defect densities.[17] In this process, the measured excess charge-carrier density was fit to a single-exponential decay:

$$A = y_o + ae^{-t/\tau} \quad (1)$$

The extracted lifetimes, τ, were converted to surface recombination velocities, S, using

$$\frac{1}{\tau} = \frac{1}{\tau_B} + \frac{2S}{d} \quad (2)$$

where τ and τ_B are the measured lifetime and the bulk lifetime, respectively, and d is the thickness of the Si wafer. Because τ is much less than τ_B, eq 2 can be simplified, yielding

$$S = \frac{d}{2\tau} \quad (3)$$

A consistent trend (Figure 4) was observed for S as a function of $\chi_{CH_2CHCH_2MgCl}$. $CH_3-Si(111)$ surfaces had consistently lower S values than $CH_2CHCH_2-Si(111)$ surfaces, with MM-Si(111) samples having intermediate values of S.

D. Oxidation in Air. The passivation toward oxidation of MM-Si(111) surfaces upon exposure to air was measured using XPS by monitoring the SiO_x peak at ~102.5 eV. The air oxidation in the dark of MM-Si(111) surfaces was compared to that of $CH_3-Si(111)$ and $CH_2CHCH_2-Si(111)$ (Figure 5). After 4 weeks in air, the $CH_2CHCH_2-Si(111)$ surface exhibited approximately 0.2 MLs of SiO_x, whereas after that same time period, the SiO_x peak observed on the $CH_3-Si(111)$ was too small to be fit using the XPS analysis software. MM-Si(111) surfaces prepared from solutions having $\chi_{CH_2CHCH_2MgCl} = 0.02$ exhibited oxidation behavior that was essentially the same as that of the $CH_3-Si(111)$ surface, whereas surfaces prepared from solutions having $\chi_{CH_2CHCH_2MgCl} = 0.10$ showed observable oxide after 2 weeks in air, and <0.1 ML of SiO_x after 4 weeks in air.

IV. Discussion

The formation of MM-Si(111) surfaces from reaction solutions having $\chi_{CH_2CHCH_2MgCl} \leq 0.10$ resulted in an increase in θ_{Si-C} relative to that of the $CH_2CHCH_2-Si(111)$ surface. On the basis of previous work, atop sites that were not terminated by an organic group are most likely to be H-terminated.[34,40]

The value of S increased approximately linearly with $\chi_{CH_2CHCH_2MgCl}$. Thus, the smallest values of S were observed for the pure methyl monolayer surfaces. However, the surface recombination velocities of the MM-Si(111) surfaces were also very low, and tended toward those of the pure $CH_3-Si(111)$. None of the surface recombination velocities measured in this work would contribute significantly to electron−hole recombination in an actual device; however, the MM technique clearly produced surfaces with electrical recombination properties that closely resembled those of $CH_3-Si(111)$, while allowing for incorporation of a functional group component in the monolayer.

A second effect of the increase in θ_{Si-C} on the MM-Si(111) surfaces is the reduced rate of oxidation of these surfaces compared to the $CH_2CHCH_2-Si(111)$ surface. One proposed mechanism for silicon oxidation involves $H-Si(111)$ sites.[41,42] In studies of the oxidation of alkylated Si(111) surfaces, Si−C bonds have been shown to be much more kinetically stable in air than Si−H bonds.[43] The MM-Si(111) surfaces made using solutions having $\chi_{CH_2CHCH_2MgCl} = 0.02$ showed θ_{Si-C} near 1. After 4 weeks in air, these MM-Si(111) surfaces ($\chi_{CH_2CHCH_2MgCl} = 0.02$) were indistinguishable from the $CH_3-Si(111)$ surfaces in terms of SiO_x formation, despite having $\theta_{Si\text{-}CH_2CHCH_2} \approx 0.30$. We attribute this behavior to the higher θ_{Si-C} of the MM-Si(111) surface relative to the $CH_2CHCH_2-Si(111)$ surface.

The composition of the MM-Si(111) surfaces obtained from the two-step chlorination/alkylation process is likely governed by the relative reaction kinetics of the CH_2CHCH_2MgCl and CH_3MgCl Grignard reagents with the $Cl-Si(111)$ surface, rather than by steric or van der Waals interactions, or by diffusion kinetics to the surface. Both the GATR-FTIR spectra of Figure 2 and the transmission absorption trend of Figure S2 show that the surface composition is likely not linearly dependent on the composition of the reaction solution. Addition of the more bulky

CH_2CHCH_2- group was observed to be preferred over that of the smaller CH_3- group, despite the higher surface strain induced by the CH_2CHCH_2- group.[20] This behavior is consistent with kinetic control of the surface composition due to the faster kinetics of the reaction of the surface with CH_2CHCH_2MgCl than with CH_3MgCl, assuming that once terminated by an organic group, Si sites are inert to exchange. Consistently, the reaction of CH_2CHCH_2MgCl with the Cl−Si(111) surface went to near completion in less than 10 min, while the reaction of CH_3MgCl with the same surface required >30 min to approach completion.

MMs on silicon may thus exhibit benefits such as increased total surface coverage (θ_{Si-C}), superior passivation, decreased defect density, and, assuming a random distribution of functional groups, dilution of functional groups for higher-yielding secondary chemistry. A practical method to synthesize mixed allyl/methyl monolayers with controlled composition has been demonstrated, and MM-Si(111) surfaces made from solutions having $\chi_{CH_2CHCH_2MgCl} < 0.20$ have a majority of atop sites terminated by methyl groups.

V. Conclusions

MMs consisting of methyl and allyl groups have been prepared on Si(111) surfaces. GATR-FTIR spectroscopy has been used to confirm the presence of both CH_3- and CH_2CHCH_2- groups on the resulting methyl/allyl-Si(111) surfaces. The total surface coverage (θ_{Si-C}), *S* values, and surface oxidation rates of MM-Si(111) surfaces were close to those of the CH_3-Si(111) surfaces, demonstrating that it is possible to preserve the beneficial properties of the CH_3-Si(111) while incorporating a significant fraction of functional groups to allow secondary reactivity. The procedure described herein allows for the synthesis of mixed organic group surfaces that have high total surface coverages, low surface recombination velocities, and the potential for secondary functionalization, while yielding surfaces that are not limited in composition to those based upon thermodynamic considerations from sterics alone.

Acknowledgment. This work was supported by the National Science Foundation (CHE-0911682), BP, and the Molecular Materials Research Center of the Beckman Institute at the California Institute of Technology. The authors acknowledge Dr. Kate Plass, Dr. Shannon Boettcher, and Mr. Andrey Poletayev for insightful discussions.

Supporting Information Available: Details of the XPS data workup, absolute transmission of the GATR setup, and statistical analysis of XPS and transmission FTIR data. This material is available free of charge via the Internet at http://pubs.acs.org.

References and Notes

(1) Buriak, J. M. *Chem. Commun.* **1999**, 1051–1060.
(2) Buriak, J. M. *Chem. Rev.* **2002**, *102*, 1271–1308.
(3) Yates, J. T. *Science* **1998**, *279*, 335–336.
(4) Teplyakov, A. V.; Kong, M. J.; Bent, S. F. *J. Am. Chem. Soc.* **1997**, *119*, 11100–11101.
(5) Linford, M. R.; Chidsey, C. E. D. *J. Am. Chem. Soc.* **1993**, *115*, 12631–12632.
(6) Linford, M. R.; Fenter, P.; Eisenberger, P. M.; Chidsey, C. E. D. *J. Am. Chem. Soc.* **1995**, *117*, 3145–3155.
(7) Sieval, A. B.; Demirel, A. L.; Nissink, J. W. M.; Linford, M. R.; van der Maas, J. H.; de Jeu, W. H.; Zuilhof, H.; Sudholter, E. J. R. *Langmuir* **1998**, *14*, 1759–1768.
(8) Terry, J.; Linford, M. R.; Wigren, C.; Cao, R. Y.; Pianetta, P.; Chidsey, C. E. D. *Appl. Phys. Lett.* **1997**, *71*, 1056–1058.
(9) Stewart, M. P.; Buriak, J. M. *Angew. Chem., Int. Ed.* **1998**, *37*, 3257–3260.
(10) Lewis, L. N. *J. Am. Chem. Soc.* **1990**, *112*, 5998–6004.
(11) Bansal, A.; Li, X. L.; Lauermann, I.; Lewis, N. S.; Yi, S. I.; Weinberg, W. H. *J. Am. Chem. Soc.* **1996**, *118*, 7225–7226.
(12) Allongue, P.; Delamar, M.; Desbat, B.; Fagebaume, O.; Hitmi, R.; Pinson, J.; Saveant, J. M. *J. Am. Chem. Soc.* **1997**, *119*, 201–207.
(13) Niederhauser, T. L.; Jiang, G. L.; Lua, Y. Y.; Dorff, M. J.; Woolley, A. T.; Asplund, M. C.; Berges, D. A.; Linford, M. R. *Langmuir* **2001**, *17*, 5889–5900.
(14) Pike, A. R.; Lie, L. H.; Eagling, R. A.; Ryder, L. C.; Patole, S. N.; Connolly, B. A.; Horrocks, B. R.; Houlton, A. *Angew. Chem., Int. Ed.* **2002**, *41*, 615–617.
(15) Strother, T.; Cai, W.; Zhao, X. S.; Hamers, R. J.; Smith, L. M. *J. Am. Chem. Soc.* **2000**, *122*, 1205–1209.
(16) Fabre, B.; Lopinski, G. P.; Wayner, D. D. M. *J. Phys. Chem. B* **2003**, *107*, 14326–14335.
(17) Royea, W. J.; Juang, A.; Lewis, N. S. *Appl. Phys. Lett.* **2000**, *77*, 1988–1990.
(18) Hunger, R.; Fritsche, R.; Jaeckel, B.; Jaegermann, W.; Webb, L. J.; Lewis, N. S. *Phys. Rev. B* **2005**, *72*, 045317.
(19) Yu, H. B.; Webb, L. J.; Ries, R. S.; Solares, S. D.; Goddard, W. A.; Heath, J. R.; Lewis, N. S. *J. Phys. Chem. B* **2005**, *109*, 671–674.
(20) Nemanick, E. J.; Solares, S. D.; Goddard, W. A.; Lewis, N. S. *J. Phys. Chem. B* **2006**, *110*, 14842–14848.
(21) Maldonado, S.; Plass, K. E.; Knapp, D.; Lewis, N. S. *J. Phys. Chem. C* **2007**, *111*, 17690–17699.
(22) Juang, A.; Scherman, O. A.; Grubbs, R. H.; Lewis, N. S. *Langmuir* **2001**, *17*, 1321–1323.
(23) Plass, K. E.; Liu, X. L.; Brunschwig, B. S.; Lewis, N. S. *Chem. Mater.* **2008**, *20*, 2228–2233.
(24) Rohde, R. D.; Agnew, H. D.; Yeo, W. S.; Bailey, R. C.; Heath, J. R. *J. Am. Chem. Soc.* **2006**, *128*, 9518–9525.
(25) Dutta, S.; Perring, M.; Barrett, S.; Mitchell, M.; Kenis, P. J. A.; Bowden, N. B. *Langmuir* **2006**, *22*, 2146–2155.
(26) Faucheux, A.; Gouget-Laemmel, A. C.; de Villeneuve, C. H.; Boukherroub, R.; Ozanam, F.; Allongue, P.; Chazalviel, J. N. *Langmuir* **2006**, *22*, 153–162.
(27) Sun, Q. Y.; de Smet, L.; van Lagen, B.; Giesbers, M.; Thune, P. C.; van Engelenburg, J.; de Wolf, F. A.; Zuilhof, H.; Sudholter, E. J. R. *J. Am. Chem. Soc.* **2005**, *127*, 2514–2523.
(28) Liu, Y. J.; Navasero, N. M.; Yu, H. Z. *Langmuir* **2004**, *20*, 4039–4050.
(29) Boukherroub, R.; Wayner, D. D. M. *J. Am. Chem. Soc.* **1999**, *121*, 11513–11515.
(30) Offord, D. A.; Griffin, J. H. *Langmuir* **1993**, *9*, 3015–3025.
(31) Mathauer, K.; Frank, C. W. *Langmuir* **1993**, *9*, 3002–3008.
(32) Heise, A.; Stamm, M.; Rauscher, M.; Duschner, H.; Menzel, H. *Thin Solid Films* **1998**, *327*, 199–203.
(33) Fabre, B.; Hauquier, F. *J. Phys. Chem. B* **2006**, *110*, 6848–6855.
(34) Nemanick, E. J.; Hurley, P. T.; Brunschwig, B. S.; Lewis, N. S. *J. Phys. Chem. B* **2006**, *110*, 14800–14808.
(35) Amy, S. R.; Michalak, D. J.; Chabal, Y. J.; Wielunski, L.; Hurley, P. T.; Lewis, N. S. *J. Phys. Chem. C* **2007**, *111*, 13053–13061.
(36) Higashi, G. S.; Chabal, Y. J.; Trucks, G. W.; Raghavachari, K. *Appl. Phys. Lett.* **1990**, *56*, 656–658.
(37) Bansal, A.; Li, X. L.; Yi, S. I.; Weinberg, W. H.; Lewis, N. S. *J. Phys. Chem. B* **2001**, *105*, 10266–10277.
(38) Webb, L. J.; Rivillon, S.; Michalak, D. J.; Chabal, Y. J.; Lewis, N. S. *J. Phys. Chem. B* **2006**, *110*, 7349–7356.
(39) Milosevic, M.; Milosevic, V.; Berets, S. L. *Appl. Spectrosc.* **2007**, *61*, 530–536.
(40) Johansson, E.; Hurley, P. T.; Brunschwig, B. S.; Lewis, N. S. *J. Phys. Chem. C* **2009**, *113*, 15239–15245.
(41) Cicero, R. L.; Linford, M. R.; Chidsey, C. E. D. *Langmuir* **2000**, *16*, 5688–5695.
(42) Neuwald, U.; Hessel, H. E.; Feltz, A.; Memmert, U.; Behm, R. J. *Appl. Phys. Lett.* **1992**, *60*, 1307–1309.
(43) Webb, L. J.; Michalak, D. J.; Biteen, J. S.; Brunschwig, B. S.; Chan, A. S. Y.; Knapp, D. W.; Meyer, H. M.; Nemanick, E. J.; Traub, M. C.; Lewis, N. S. *J. Phys. Chem. B* **2006**, *110*, 23450–23459.

JP911379C